PROCEEDINGS OF SCIENCE

Modelling Pulsar Gamma-ray Light Curves using a Geometric Current Sheet Model

C Venter,[a,*] **A Harding,**[b] **C Kalapotharakos**[c] **and TM Nyambe**[a]

[a] *Centre for Space Research, North-West University, Private Bag X6001, Potchefstroom 2520, South Africa*
[b] *Theoretical Division, Los Alamos National Laboratory, Los Alamos, NM 87545*
[c] *Astrophysics Science Division, NASA Goddard Space Flight Center, Greenbelt, MD 20771, USA*

E-mail: Christo.Venter@nwu.ac.za

The publication of the Third Pulsar Catalog (3PC) by the *Fermi* Large Area Telescope (LAT) team marked a significant milestone for high-energy pulsar science. In it, the light curves and spectra of nearly 300 pulsars are presented, along with some interesting correlations between timing and spectral parameters. This wealth of data provides impetus for continued development of pulsar emission models. Over the years, numerous models have been developed, focusing on different physical aspects or regimes (e.g., global current flow and magnetic field structure, pair creation microphysics, or emission and beaming), and with different outputs (e.g., multi-frequency light curves, multi-component spectra, or single-band pulse shapes only). Magnetohydrodynamic (MHD) and particle-in-cell (PIC) models each have their respective strengths but are often computationally expensive for a suitable coverage of the parameter space. Machine learning has recently been invoked to speed up the process. An alternative, interim step that we are exploring is to implement a geometric current sheet (CS) model, akin to the traditional outer gap and two-pole caustic models, but with emission occurring beyond the light cylinder (the magnetospheric boundary where the co-rotation speed equals that of light in vacuum). We present first results and insights gained by evaluating the beamed output (phase plots or sky maps that present beamed emission across the sky) from this model, as well as from contrasting example predicted light curves for the Vela pulsar using the various geometric models. The latter results also feature predictions from a geometric radio conal model.

High Energy Astrophysics in Southern Africa (HEASA2025)
16-20 September, 2025
University of Johannesburg, South Africa

*Speaker

 ISSN 1824-8039 . Published by SISSA Medialab.

PoS(HEASA2025)058

1. Introduction

The publication of the Third Pulsar Catalog (3PC) by the *Fermi* Large Area Telescope (LAT) team contains 294 gamma-ray pulsars, 33 gamma-ray candidates, and 12 optical / X-ray candidates [1]. This is a tremendous increase with respect to the $\sim$ 10 known gamma-ray pulsars before the launch of *Fermi*. A number of interesting discoveries including a diversity of pulse profile shapes, no apparent correlation between the radio and gamma-ray fluxes, relatively harder second peaks (i.e., a decreasing ratio of the fluxes of peak one versus peak two with energy), relatively more curved spectra for lower-spin-down (older) pulsars, and an inverse trend between the gamma-ray peak separation (Δ) versus phase offset between the radio and gamma-ray pulses (δ), underscore the rich phenomenology that models have to capture. Geometric two-pole-caustic (TPC) and outer gap (OG) models have in the past been used to model gamma-ray pulsar light curves [2].

With regards to magnetic field structure, an early vacuum retarded dipole (RVD) by [3] has been used. Ideal magnetohydrodynamic (MHD) models yielded force-free (FF) magnetospheres (plasma-filled ones with no accelerating electric field), both in the spin-aligned case and non-aligned rotation ($\boldsymbol{\Omega}$) and magnetic dipole ($\boldsymbol{\mu}$) axes case [4–6]. Dissipative MHD solutions [7–10] included deviations from local FF regimes. Emission models invoking various radiation processes within FF magnetospheres have been used to study the broadband spectra of some pulsars [11, 12], while the particle flow and acceleration microphysics have been studied using global particle-in-cell (PIC) codes [13–23]. A recent novel model includes aspects of magnetospheric geometry and synchro-curvature emission physics, and is able to produce light curves and spectra using only a few parameters [24]. For a review of pulsar models, refer to [25].

While earlier models ascribed emission to regions within the light cylinder at a radius $R_{\rm LC}$, PIC models indicated that for increased particle (secondary pair) injection rates, the dominant dissipation regions are relegated to the equatorial current sheet (CS) beyond $R_{\rm LC}$, e.g., [18, 19]. Moreover, the CS is also shown to be the dominant region of emission by dissipative MHD codes, e.g., [9, 17]. This was confirmed by a hybrid PIC-MHD model [26]. The CS geometry predicts ubiquitous double-peaked/caustic gamma-ray light-curve morphologies, while being able to reproduce the δ–Δ correlation (radio-gamma lag vs gamma peak separation) [9]. Finally, the predicted spectra and energetics are broadly consistent with gamma-ray observations after scaling up the artificially low PIC fields to realistic pulsar fields. These facts have led to a consensus view that the CS emission region is a viable generic theoretical framework to explain high-energy pulsar emission, although details of pair injection, reconnection physics, and emissivity prescriptions remain open.

While the theoretical pulsar programme has made significant strides, the MHD, PIC, and emission models mentioned above are typically computationally very costly to run. This implies that parameter space may not be adequately explored due to long run times. Machine learning techniques may aid in speeding up the models (by extrapolating from the outputs of simpler models to those of computationally intensive ones via the use of a surrogate model), and thereby opening up parameter space [27]. In this paper, we take an alternative approach, leveraging the theoretical insights brought by the sophisticated emission models and the speed of geometrical models. The latter assume a particular magnetic field geometry and a distribution of emission on these field lines, focusing on the correct beaming of the emission and thereby yielding phaseplots (intensity versus observer angle ζ and rotational phase ϕ) and light curves, but no spectral predictions. This

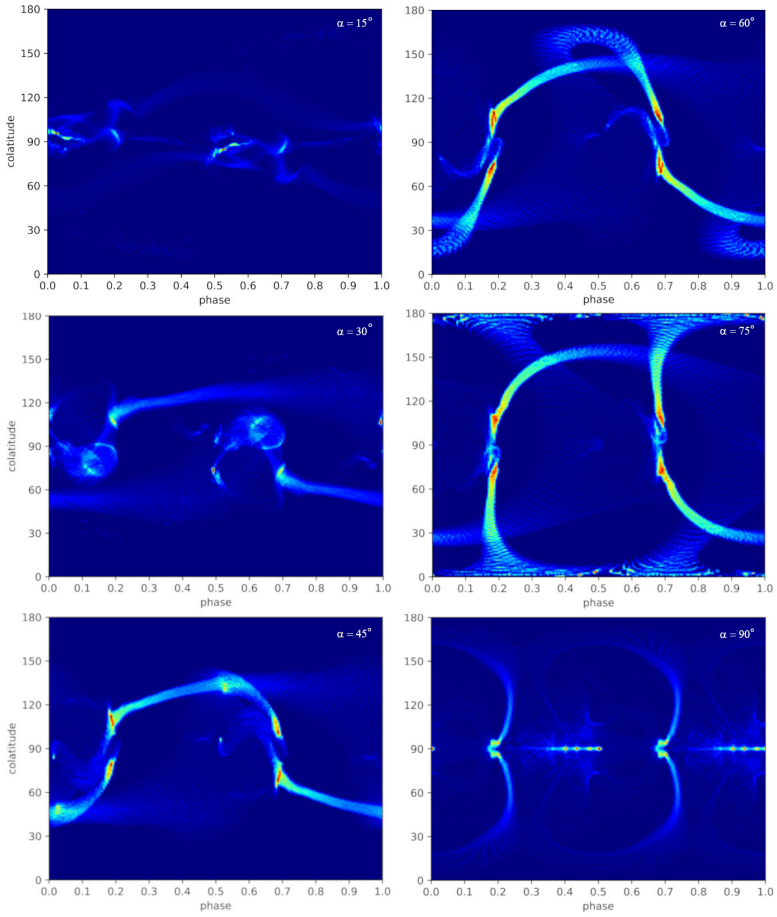

Figure 1: Phaseplots from the geometric CS model, with α as indicated in the top right corner of each panel. This is for an FF magnetic field. Other parameters include open-volume radial coordinates (akin to a scaled polar angle, being unity at the polar cap rim) of $(\xi_{\rm in}, \xi_{\rm out}) = (0.90, 0.96)$ and a radial extent of $(R_{\rm in}, R_{\rm out}) = (1.0, 1.5)R_{\rm LC}$.

is to facilitate inference of pulsar geometries (magnetic inclination angle α and ζ), similar to what was done by [28–31], without attempting to explain other radiative properties, and invoking an FF magnetic field. Below, we describe our implementation of a geometrical current-sheet model (Section 2), some first results of this model (Section 3), and our conclusions follow in Section 4.

2. Model

Some older geometric radio / OG / TPC models [2] invoked an analytic retarded vacuum dipole (RVD) magnetic field, performed their calculations in the co-rotating frame (or lab frame) up to the light cylinder, and included no emission physics (and thus no spectral outputs). The ones calculated in the co-rotating frame implemented a Lorentz transformation to the lab frame to obtain the correct beaming. On the other hand, emission models [12, 32] typically import numerical FF magnetic fields, the calculations are performed in the lab frame, the emission extends beyond the light cylinder, and the inclusion of emission physics yield predictions of spectra and energy-dependent light curves.

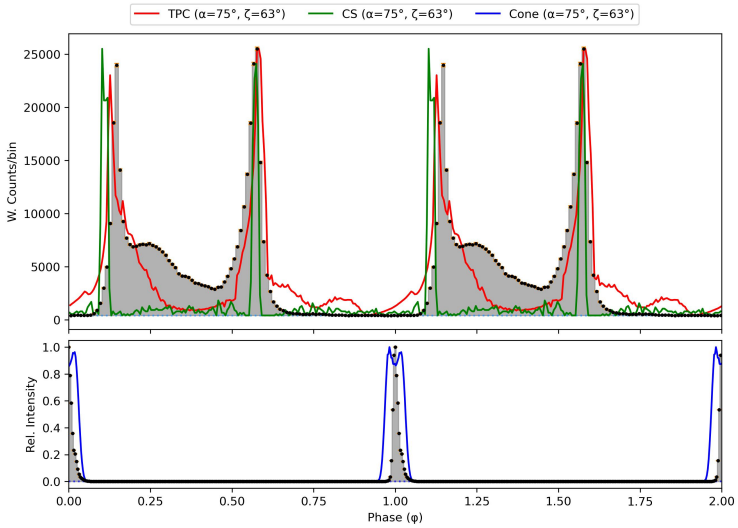

Figure 2: Examples of radio and gamma-ray light curves for the Vela pulsar using the geometric TPC and CS models, as well as a conal radio model [33].

In this paper, we take the best of both worlds, but with the view of speeding up the calculation. Our geometric CS model thus incorporates a realistic numerical FF magnetic field, the calculations are performed in the lab frame (allowing us to place emission beyond the light cylinder); but no emission physics is included.

3. Results

Figure 1 indicates phaseplots from the CS model for an FF magnetosphere for the range of $\alpha \in (15°, 30°, 45°, 60°, 75°, 90°)$. One may see the caustics that form near the equator for small α but that 'rotates' and become more vertical and spread out as α increases. We set the inner and outer open-volume radial coordinate that delineate the (cross-sectional) boundaries of the separatrix (gap) on the stellar surface [34] to[1] $(\xi_{\rm in}, \xi_{\rm out}) = (0.90, 0.96)$, while we chose the minimum and maximum gap radius to be $(R_{\rm in}, R_{\rm out}) = (1.0, 1.5)R_{\rm LC}$. These caustics resemble those of other works [6, 9, 35].

In Figure 2, we indicate example radio and gamma-ray model light curves for the Vela pulsar (illustrative, not a formal fit), using both the traditional TPC and the geometric CS model as well as a conal radio model [33] for $\alpha = 75°$ and $\zeta = 63°$ (given our current grid in α for the imported FF field). We note that the CS model predicts two peaks at nearly the right phases, but they are very narrow; in future, we will explore changing the sheet thickness or even including some emission from below the light cylinder to improve the model prediction. The TPC captures more of the gamma-ray peak shape, but underpredicts some emission of the third peak (P3). The radio peak is also too wide and indicates a dip at this (α, ζ) combination. In future, a more detailed fitting approach will be implemented to exhaustively search parameter space and formally derive best-fit parameters. We may also use the test statistic developed by A.S. Seyffert [36] to perform joint

[1]The ξ is roughly a dimensionless polar angle going from 0 at the magnetic axis to 1 at the PC rim.

fitting where the radio and gamma-ray contributions are balanced, despite the relative difference in error across these wavebands.

4. Conclusions

There is a wealth of new data on gamma-ray pulsars. Theorists are reaching for an overarching model framework to explain the rich phenomenology. This follows decades of model development using different approaches. Computationally expensive models may inhibit exhaustive searches of parameter space for best-fit solutions to the data. In this paper, we motivated the development of an interim geometric CS gamma-ray pulsar model, with emission occurring beyond the light cylinder. This is a practical measure to facilitate the routine joint fitting of radio and gamma-ray light curves, while more sophisticated models and techniques are being refined. We presented first example results. It seems that the resulting pulsar parameters may not be too different from those inferred by traditional models, although more study is needed to confirm this. If true, this means that the former models may be used as an approximation of newer models, especially for quick-look results. This is because the caustic that develops in the CS model is roughly akin to an adjacent layer of emission compared to that predicted by the OG and TPC models, while we use the same radio model. Implementation of machine learning to speed up the calculations of realistic emission models will facilitate an adequate exploration of parameter space, something that has not been possible until now. In this context, our geometric CS model may act as a bridge and provide a sanity check during the development phase of such techniques.

Acknowledgements

This work is based on research supported wholly/in part by the National Research Foundation of South Africa (NRF). The Grant holder acknowledges that opinions, findings and conclusions or recommendations expressed in any publication generated by the NRF-supported research is that of the author(s), and that the NRF accepts no liability whatsoever in this regard. Resources supporting this work were provided by the NASA High-End Computing (HEC) Program through the NASA Advanced Supercomputing (NAS) Division at Ames Research Center.

References

[1] D.A. Smith, S. Abdollahi, M. Ajello, M. Bailes et al., *The Third Fermi Large Area Telescope Catalog of Gamma-Ray Pulsars*, *ApJ* **958** (2023) 191.

[2] C. Venter, A.K. Harding and L. Guillemot, *Probing Millisecond Pulsar Emission Geometry Using Light Curves from the Fermi/Large Area Telescope*, *ApJ* **707** (2009) 800.

[3] A.J. Deutsch, *The Electromagnetic Field of an Idealized Star in Rigid Rotation in Vacuo*, *Annales d'Astrophysique* **18** (1955) 1.

[4] I. Contopoulos, D. Kazanas and C. Fendt, *The Axisymmetric Pulsar Magnetosphere*, *ApJ* **511** (1999) 351.

[5] A. Spitkovsky, *Time-dependent Force-free Pulsar Magnetospheres: Axisymmetric and Oblique Rotators*, *ApJL* **648** (2006) L51.

[6] X.-N. Bai and A. Spitkovsky, *Modeling of Gamma-ray Pulsar Light Curves Using the Force-free Magnetic Field*, *ApJ* **715** (2010) 1282.

[7] C. Kalapotharakos, A.K. Harding, D. Kazanas and I. Contopoulos, *Gamma-Ray Light Curves from Pulsar Magnetospheres with Finite Conductivity*, *ApJL* **754** (2012) L1.

[8] J. Li, A. Spitkovsky and A. Tchekhovskoy, *Resistive Solutions for Pulsar Magnetospheres*, *ApJ* **746** (2012) 60.

[9] C. Kalapotharakos, A.K. Harding and D. Kazanas, *Gamma-Ray Emission in Dissipative Pulsar Magnetospheres: From Theory to Fermi Observations*, *ApJ* **793** (2014) 97.

[10] G. Brambilla, C. Kalapotharakos, A.K. Harding and D. Kazanas, *Testing Dissipative Magnetosphere Model Light Curves and Spectra with Fermi Pulsars*, *ApJ* **804** (2015) 84.

[11] A.K. Harding, C. Kalapotharakos, M. Barnard and C. Venter, *Multi-TeV Emission from the Vela Pulsar*, *ApJL* **869** (2018) L18.

[12] A.K. Harding, C. Venter and C. Kalapotharakos, *Very-high-energy Emission from Pulsars*, *ApJ* **923** (2021) 194.

[13] A.Y. Chen and A.M. Beloborodov, *Electrodynamics of Axisymmetric Pulsar Magnetosphere with Electron-Positron Discharge: A Numerical Experiment*, *ApJL* **795** (2014) L22.

[14] A.A. Philippov and A. Spitkovsky, *Ab Initio Pulsar Magnetosphere: Three-dimensional Particle-in-cell Simulations of Axisymmetric Pulsars*, *ApJL* **785** (2014) L33.

[15] A.A. Philippov, A. Spitkovsky and B. Cerutti, *Ab Initio Pulsar Magnetosphere: Three-dimensional Particle-in-cell Simulations of Oblique Pulsars*, *ApJL* **801** (2015) L19.

[16] A.A. Philippov, B. Cerutti, A. Tchekhovskoy and A. Spitkovsky, *Ab Initio Pulsar Magnetosphere: The Role of General Relativity*, *ApJL* **815** (2015) L19.

[17] A.A. Philippov and A. Spitkovsky, *Ab-initio Pulsar Magnetosphere: Particle Acceleration in Oblique Rotators and High-energy Emission Modeling*, *ApJ* **855** (2018) 94.

[18] B. Cerutti, A.A. Philippov and A. Spitkovsky, *Modelling High-energy Pulsar Light Curves from First Principles*, *MNRAS* **457** (2016) 2401.

[19] G. Brambilla, C. Kalapotharakos, A.N. Timokhin, A.K. Harding and D. Kazanas, *Electron-Positron Pair Flow and Current Composition in the Pulsar Magnetosphere*, *ApJ* **858** (2018) 81.

[20] C. Kalapotharakos, G. Brambilla, A. Timokhin, A.K. Harding and D. Kazanas, *Three-dimensional Kinetic Pulsar Magnetosphere Models: Connecting to Gamma-Ray Observations*, *ApJ* **857** (2018) 44.

[21] B. Cerutti, A.A. Philippov and G. Dubus, *Dissipation of the Striped Pulsar Wind and Non-thermal Particle Acceleration: 3D PIC Simulations*, *A&A* **642** (2020) A204.

[22] C. Kalapotharakos, Z. Wadiasingh, A.K. Harding and D. Kazanas, *The Gamma-Ray Pulsar Phenomenology in View of 3D Kinetic Global Magnetosphere Models*, *ApJ* **954** (2023) 204.

[23] B. Cerutti, E. Figueiredo and G. Dubus, *Synthetic Pulsar Light Curves from Global Kinetic Simulations and Comparison with the Fermi-LAT Catalog*, *A&A* **695** (2025) A93.

[24] D. Íñiguez-Pascual, D.F. Torres and D. Viganò, *Synchro-curvature Description of γ-ray Light Curves and Spectra of Pulsars: Global Properties*, *MNRAS* **530** (2024) 1550.

[25] A. Philippov and M. Kramer, *Pulsar Magnetospheres and Their Radiation*, *Ann. Rev. Astron. Astrophys.* **60** (2022) 495.

[26] A. Soudais, B. Cerutti and I. Contopoulos, *Scaling up Global Kinetic Models of Pulsar Magnetospheres using a Hybrid Force-free-PIC Numerical approach*, *A&A* **690** (2024) A170.

[27] G. Olmschenk, E. Broadbent, C. Kalapotharakos, W.F. Wallace, T. Lechien, Z. Wadiasingh et al., *Pioneering High-speed Pulsar Parameter Estimation Using Convolutional Neural Networks*, *ApJ* **991** (2025) 169.

[28] O. Benli, J. Pétri and D. Mitra, *Constraining Millisecond Pulsar Geometry Using Time-aligned Radio and Gamma-ray Pulse Profile*, *A&A* **647** (2021) A101.

[29] J. Pétri and D. Mitra, *Young Radio-loud Gamma-ray Pulsar Light Curve Fitting*, *A&A* **654** (2021) A106.

[30] J. Pétri, *Multi-wavelength Pulse Profiles from the Force-free Neutron Star Magnetosphere*, *A&A* **687** (2024) A169.

[31] J. Pétri, S. Guillot, L. Guillemot, D. González-Caniulef, F. Jankowski, J.M. Grießmeier et al., *A Double Dipole Geometry for PSR J0740+6620*, *A&A* **701** (2025) A39.

[32] M. Barnard, C. Venter, A.K. Harding, C. Kalapotharakos and T.J. Johnson, *Probing the High-energy Gamma-Ray Emission Mechanism in the Vela Pulsar via Phase-resolved Spectral and Energy-dependent Light-curve Modeling*, *ApJ* **925** (2022) 184.

[33] S.A. Story, P.L. Gonthier and A.K. Harding, *Population Synthesis of Radio and γ-Ray Millisecond Pulsars from the Galactic Disk*, *ApJ* **671** (2007) 713.

[34] J. Dyks, A.K. Harding and B. Rudak, *Relativistic Effects and Polarization in Three High-Energy Pulsar Models*, *ApJ* **606** (2004) 1125.

[35] J. Pétri, *Radiative Pulsar Magnetospheres: Oblique Rotators*, *MNRAS* **512** (2022) 2854.

[36] A. Corongiu, R.P. Mignani, A.S. Seyffert et al., *Radio Pulsations from the γ-ray Millisecond Pulsar PSR J2039-5617*, *MNRAS* **502** (2021) 935.